
A Modern Take on the Bias-Variance Tradeoff in Neural Networks

Brady Neal¹ Sarthak Mittal¹ Aristide Baratin¹ Vinayak Tantia¹ Matthew Scicluna¹
Simon Lacoste-Julien¹ Ioannis Mitliagkas¹

Abstract

We revisit the bias-variance tradeoff for neural networks in light of modern empirical findings. The traditional bias-variance tradeoff in machine learning suggests that as model capacity grows, bias decreases and variance increases. In contrast, we find that *both* bias *and* variance can decrease with the number of parameters. To better understand this, we decompose the total variance into variance due to training set sampling and variance due to initialization. Surprisingly, variance due to training set sampling is roughly constant with both network width and depth, in the over-parameterized setting. We provide theoretical analysis, in a simplified setting inspired by linear models, that is consistent with our empirical findings.

1. Introduction

The traditional view in machine learning is that increasingly complex models achieve lower bias at the expense of higher variance. This balance between underfitting (high bias) and overfitting (high variance) is commonly known as the *bias-variance tradeoff* (Fig. 1). In their landmark work that highlighted this bias-variance dilemma in machine learning, Geman et al. (1992) suggest that bias decreases and variance increases with network size. Because bias and variance contribute to test set performance (through the bias-variance decomposition), this provided strong intuition for how we think about generalization capabilities of large models. Learning theory supports this intuition, as most classical and current bounds on generalization error grow with the size of the networks.

However, there is a growing amount of evidence of *larger* networks generalizing *better* than their smaller counterparts in practice (Neyshabur et al., 2015; Novak et al., 2018;

¹Mila, Université de Montréal. Correspondence to: Brady Neal <bradyneal11@gmail.com>.

Zhang et al., 2017; Canziani et al., 2016). This apparent mismatch between theory and practice is due to the use of worst-case analysis that depends only on the model class, completely agnostic to data distribution and without taking optimization into account. Some recent work has gone in the direction of taking this information into account (Neyshabur, 2017; Neyshabur et al., 2019; Kuzborskij & Lampert, 2018; Dziugaite & Roy, 2017). A modern empirical study of bias-variance can take all of this information into account.

We revisit the bias-variance tradeoff in the modern setting, focusing on how variance changes when the size of neural networks increases. We test the hypothesis that “the price to pay for achieving low bias is high variance” (Geman et al., 1992). In contrast to this traditional view, we find evidence that *both* bias *and* variance decrease with network width (Fig. 1). This can be seen as the “bias-variance analog” of the described recent evidence of larger networks generalizing better. More in line with the tradeoff, we find that variance grows slowly with depth, using current best practices.

To better understand these coarse trends, we develop a new, more fine-grain method to study variance in models that depend on randomness in optimization. We separate variance due to sampling of the training set (what is normally simply referred to as “variance” in simple settings) from variance due to initialization. We find that variance due to training set sampling is roughly *constant* with both width and, surprisingly, depth (Fig. 2). Variance due to initialization decreases with width and increases with depth, in our setting (Fig. 2).

We provide simple theoretical analysis in line with our empirical findings. We point out that constant variance due to training set sampling can already be seen in over-parameterized linear models. Taking inspiration from linear models, we provide a more general result in a simplified nonlinear setting that is consistent with our empirical findings for width. We see further theoretical treatment of variance as a fruitful direction for better understanding complexity and generalization abilities of neural networks.

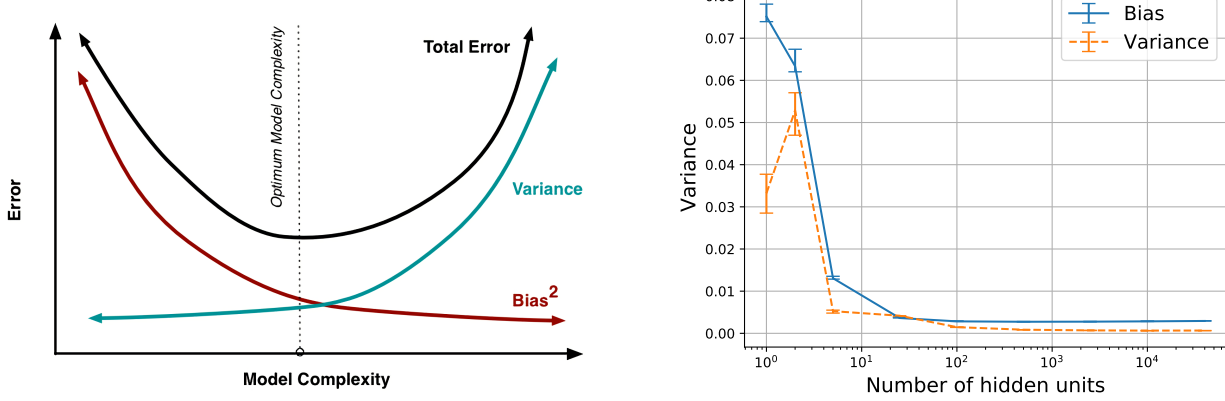


Figure 1: On the left is an illustration of the common intuition for the bias-variance tradeoff (Fortmann-Roe, 2012). We find that variance decreases along with bias when increasing network width (right). These results seem to contradict the traditional intuition.

Main Contributions

1. We revisit the bias-variance analysis in the modern setting for neural networks and point out that it is not necessarily a tradeoff as overall variance *decreases* with width (similar to bias), yielding better generalization (Fig. 1).
2. We perform a more fine-grain study of variance in neural networks by decomposing it into variance due to initialization and variance due to sampling. Variance due to sampling is roughly *constant* with both width and depth. Variance due to initialization decreases with width, while it increases with depth, in the settings we consider (Fig. 2, Section 3.4, Section 4.2).
3. We remark that this variance phenomenon is already present in over-parameterized linear models. In a simplified setting, inspired by linear models, we provide theoretical analysis in support of our empirical findings for network width (Section 5).

Most of our experiments use SGD with momentum. Interestingly, in a few experiments performed with different optimizers, we observe the same decreasing variance trend with width (Section 3.3, Appendix B.4).

1.1. Related Work

Neyshabur et al. (2015); Neyshabur (2017) point out that because increasing network width does not lead to a U-shaped test error curve, there must be some form of implicit regularization controlling capacity, e.g. due to optimization by gradient descent (Soudry et al., 2018; Gunasekar et al.,

2018a;b). Our work is consistent with this finding, but by approaching the problem from the bias-variance perspective, we gain additional insights: 1) We specifically address the hypothesis that decreased bias must come at the expense of increased variance. 2) We find that while bias does decrease with width and depth, variance actually increases with depth; our more fine-grain approach reveals the distinguishing factor between width and depth is more related to optimization (variance due to initialization) than traditional capacity control (variance due to sampling). 3) Because variance does not depend on the labels, our theoretical treatment of variance is quite different from the theoretical treatment of generalization error.

To ensure that we are studying networks of increasing capacity, one of the experimental controls we use throughout the paper is to verify that bias is decreasing along the dimension we are varying (i.e. width or depth).

In concurrent work, Spigler et al. (2018); Belkin et al. (2018) point out that generalization error acts according to conventional wisdom in the under-parameterized setting, that it decreases with capacity in the over-parameterized setting, and that there is a sharp transition between the two settings. While this transition can roughly be seen as the early hump in variance we observe in some of our graphs, we mostly focus on the over-parameterized setting. Additionally, our work is unique in that we explicitly analyze and experimentally measure the quantities of bias and variance. Interestingly, Belkin et al. (2018)'s empirical study of test error provides some evidence that our bias-variance finding might not be unique to neural networks and might be found in other models such as decision trees.

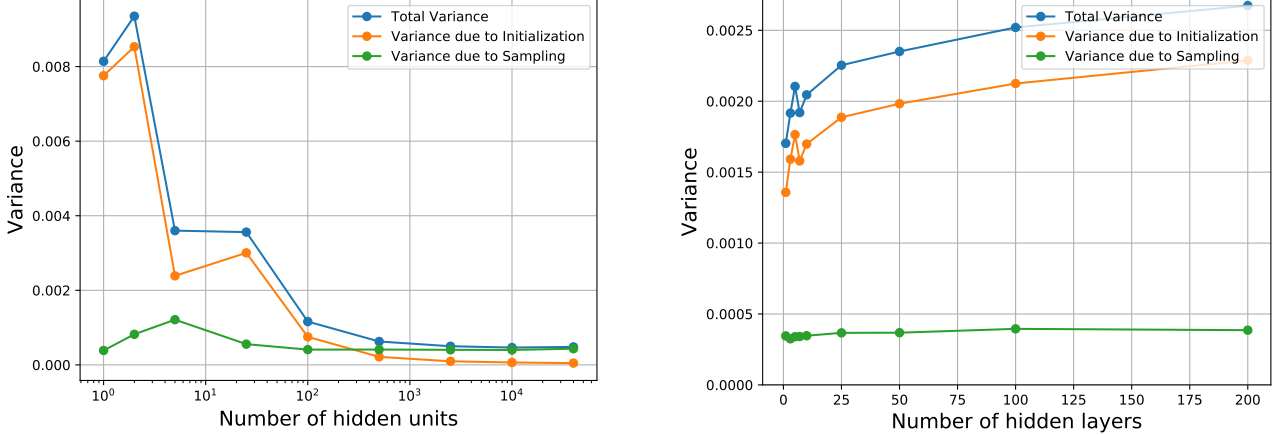


Figure 2: Trends of variance due to sampling and variance due to initialization with width (left) and with depth (right). Variance due to sampling is roughly *constant* with both width and depth, in contrast with what the bias-variance tradeoff might suggest. Variance due to initialization differentiates the effects of width and depth and is in line with neural network optimization literature.

1.2. Organization

The rest of this paper is organized as follows. Section 2 establishes necessary preliminaries. In Section 3 and Section 4, we study the impact of network width and network depth (respectively) on variance. In Section 5, we present theoretical analysis in support of our findings.

2. Preliminaries

2.1. Set-up

We consider the typical supervised learning task of predicting an output $y \in \mathcal{Y}$ from an input $x \in \mathcal{X}$, where the pairs (x, y) are drawn from some unknown joint distribution, \mathcal{D} . The learning problem consists of inferring a function $h_S : \mathcal{X} \rightarrow \mathcal{Y}$ from a finite training dataset S of m i.i.d. samples from \mathcal{D} . The quality of a predictor h can be quantified by the expected error,

$$\mathcal{E}(h) = \mathbb{E}_{(x,y) \sim \mathcal{D}} \ell(h(x), y) \quad (1)$$

for some loss function $\ell : \mathcal{Y} \times \mathcal{Y} \rightarrow \mathbb{R}$.

In this paper, predictors h_θ are parameterized by the weights $\theta \in \mathbb{R}^N$ of deep neural networks. We consider a *frequentist risk* analysis of the learning algorithm, that is, the average performance over possible training sets (denoted by the random variable S) of size m . This is the same quantity Geman et al. (1992) consider. While S is the only random quantity focused on in traditional bias-variance decomposition, we also focus on randomness coming from optimization. We denote the random variable for optimization randomness (e.g. initialization) by I .¹

¹We focus on randomness from initialization and do not focus

Formally, given a fixed training set S and fixed optimization randomness I , the learning algorithm \mathcal{A} produces $\theta = \mathcal{A}(S, I)$. Randomness in initialization translates to randomness in $\mathcal{A}(S, \cdot)$. Given a fixed training set, we encode the randomness due to I in a conditional distribution $p(\theta|S)$; marginalizing over the training set S of size m gives a marginal distribution $p(\theta) = \mathbb{E}_S p(\theta|S)$ on the weights learned by \mathcal{A} from m samples. In this context, the frequentist risk for the learning algorithm using training sets of size m can be expressed in the following ways:

$$\mathcal{R}_m = \mathbb{E}_{\theta \sim p} \mathcal{E}(h_\theta) = \mathbb{E}_S \mathbb{E}_{\theta \sim p(\cdot|S)} \mathcal{E}(h_\theta) = \mathbb{E}_S \mathbb{E}_I \mathcal{E}(h_\theta) \quad (2)$$

2.2. Bias-Variance Decomposition

We briefly recall the standard bias-variance decomposition of the frequentist risk in the case of squared-loss. We work in the context of classification, where each class $k \in \{1 \dots K\}$ is represented by a one-hot vector in \mathbb{R}^K . The predictor outputs a score or probability vector in \mathbb{R}^K . In this context, the risk in Eq. (2) decomposes into three sources of error (Geman et al., 1992):

$$\mathcal{R}_m = \mathcal{E}_{\text{noise}} + \mathcal{E}_{\text{bias}} + \mathcal{E}_{\text{variance}} \quad (3)$$

The first term is an intrinsic error term independent of the predictor; the second is a bias term:

$$\mathcal{E}_{\text{noise}} = \mathbb{E}_{(x,y)} [\|y - \bar{y}(x)\|^2],$$

on randomness from stochastic mini-batching because we found the phenomenon of decreasing variance with width persists when using *batch* gradient descent (Section 3.3, Appendix B.4).

$$\mathcal{E}_{\text{bias}} = \mathbb{E}_x [\|\mathbb{E}_\theta[h_\theta(x)] - \bar{y}(x)\|^2],$$

where $\bar{y}(x)$ denotes the expectation $\mathbb{E}[y|x]$ of y given x . The third term is the expected variance of the output predictions:

$$\begin{aligned}\mathcal{E}_{\text{variance}} &= \mathbb{E}_x \text{Var}(h_\theta(x)), \\ \text{Var}(h_\theta(x)) &= \mathbb{E}_\theta [\|(h_\theta(x) - \mathbb{E}_\theta[h_\theta(x)])\|^2],\end{aligned}$$

where the expectation over θ can be done as in Eq. (2). Finally, in the set-up of Section 2.1, the sources of variance are the choice of training set S and the choice of initialization I (encoded into the conditional $p(\cdot|S)$). By the law of total variance, we then have the further decomposition:

$$\text{Var}(h_\theta(x)) = \mathbb{E}_S [\text{Var}_I(h_\theta(x)|S)] + \text{Var}_S (\mathbb{E}_I[h_\theta(x)|S]) \quad (4)$$

We call the first term *variance due to initialization* and the second term *variance due to sampling* throughout the paper. Note that risks computed with classification losses (e.g. cross-entropy or 0-1 loss) do not have such a clean bias-variance decomposition (Domingos, 2000; James, 2003). However, it is natural to expect that bias and variance are useful indicators of the performance of the models. In fact, we show the classification risk can be bounded as 4 times the regression risk in Appendix D.4.

3. Variance and Width

In this section, we study how variance of fully connected single hidden layer networks varies with width. We provide evidence against Geman et al. (1992)'s claim that "bias falls and variance increases with the number of hidden units." To make our study as general as possible, we consider networks without regularization bells and whistles such as weight decay, dropout, or data augmentation, which Zhang et al. (2017) found to not be necessary for good generalization.

3.1. Common Experimental Details

We run experiments on different datasets: MNIST, CIFAR10, small MNIST, and a sinusoid regression task. Averages over data samples are performed by taking the training set S and creating 50 bootstrap (Efron, 1979) replicate training sets S' by sampling with replacement from S . We train 50 different neural networks for each hidden layer size using these different training sets. Then, we estimate $\mathcal{E}_{\text{bias}}$ ² and $\mathcal{E}_{\text{variance}}$ as in Section 2.2, where the population expectation \mathbb{E}_x is estimated with an average over the test set. To estimate the two terms from the law of total variance (Equation 4), we use 10 random seeds for the outer expectation

²Because we do not have access to \bar{y} , we use the labels y to estimate $\mathcal{E}_{\text{bias}}$. This is equivalent to assuming noiseless labels and is standard procedure for estimating bias (Kohavi & Wolpert, 1996; Domingos, 2000).

and 10 for the inner expectation, resulting in a total of 100 neural networks for each hidden layer size. Furthermore, we compute 99% confidence intervals for our bias and variance estimates using the bootstrap (Efron, 1979).

The networks are trained using SGD with momentum and generally run for long after 100% training set accuracy is reached (e.g. 500 epochs for full data MNIST and 10000 epochs for small data MNIST). The overall trends we find are robust to how long the networks are trained after the training error converges. The step size hyperparameter is specified in each of the sections, and the momentum hyperparameter is always set to 0.9.

3.2. Decreasing Variance in Full Data Setting

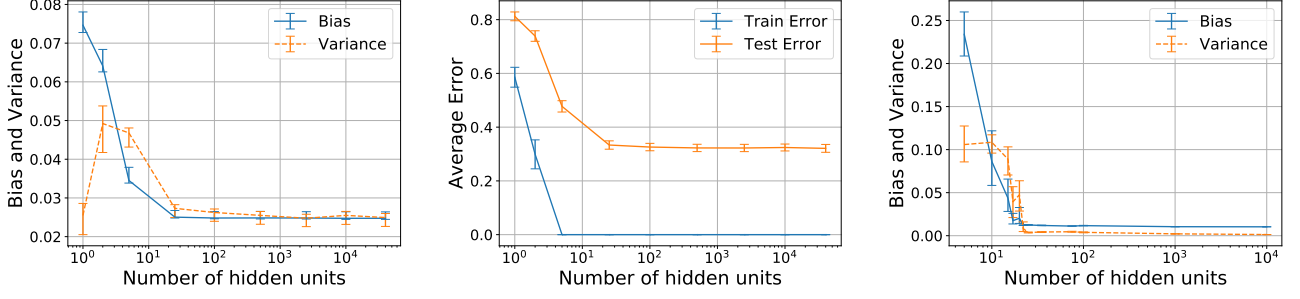
We find a clear decreasing trend in variance with width of the network in the full data MNIST setting (Fig. 1). We also see the same trend with CIFAR10 (Appendix B.1). In these experiments, the same step size is used for all networks for a given dataset (0.1 for MNIST and 0.005 for CIFAR10). The trend is the same with or without early stopping, so early stopping is not necessary to see decreasing variance, similar to how it was not necessary to see better test set performance with width in Neyshabur et al. (2015).

3.3. Testing the Limits: Decreasing Variance in the Small Data Setting

Decreasing the size of the dataset can only increase variance. To study the robustness of the above observation, we decrease the size of the training set to just 100 examples. In this small data setting, somewhat surprisingly, we still see that *both* bias and variance decrease with width (Fig. 3a). The test error behaves similarly (Fig. 3b). Because performance is more sensitive to step size in the small data setting, the step size for each network size is tuned using a validation set (see Appendix B.2 for step sizes). The training for tuning is stopped after 1000 epochs, whereas the training for the final models is stopped after 10000 epochs. Note that because we see decreasing bias with width, effective capacity is, indeed, increasing while variance is decreasing.

One control that motivates the experimental design choice of optimal step size is that it leads to the conventional decreasing bias trend (Fig. 3a) that indicates increasing effective capacity. In fact, in the corresponding experiment where step size is the same 0.01 for all network sizes, we do not see monotonically decreasing bias (Appendix B.3).

This sensitivity to step size in the small data setting is evidence that we are testing the limits of our hypothesis. By looking at the small data setting, we are able to test our hypothesis when the ratio of size of network to dataset size is quite large, and we still find this decreasing trend in vari-



(a) Variance decreases with width, even in the small MNIST setting.

(b) Test error trend is same as bias-variance trend (small MNIST).

(c) Similar bias-variance trends on sinusoid regression task.

Figure 3: We see the same bias-variance trends in small data settings: small MNIST (left) and a regression setting (right).

ance (Fig. 3a).

To see how dependent this phenomenon is on SGD, we also run these experiments using batch gradient descent and PyTorch’s version of LBFGS. Interestingly, we find a decreasing variance trend with those optimizers as well. These experiments are included in Appendix B.4.

3.4. Decoupling Variance due to Sampling from Variance due to Initialization

In order to better understand this variance phenomenon in neural networks, we separate the variance due to sampling from the variance due to initialization, according to the law of total variance (Equation 4). Contrary to what traditional bias-variance tradeoff intuition would suggest, we find variance due to sampling is roughly independent of width (Fig. 2). Furthermore, we find that variance due to initialization decreases with width, causing the joint variance to decrease with width (Fig. 2).

A body of recent work has provided evidence that over-parameterization (in width) helps gradient descent optimize to global minima in neural networks (Du et al., 2019; Du & Lee, 2018; Soltanolkotabi et al., 2017; Livni et al., 2014; Zhang et al., 2018). Always reaching a global minimum implies low variance due to initialization on the *training set*. Our observation of decreasing variance on the *test set* shows that the over-parameterization (in width) effect on optimization seems to extend to generalization, on the data sets we consider.

3.5. Visualization with Regression on Sinusoid

We trained different width neural networks on a noisy sinusoidal distribution with 80 independent training examples. This sinusoid regression setting also exhibits the familiar bias-variance trends (Fig. 3c) and trends of the two components of the variance (Fig. 5c).

Because this setting is low-dimensional, we can visualize

the learned functions. The classic caricature of high capacity models is that they fit the training data in a very erratic way (example in Fig. 13 of Appendix B.5). We find that wider networks learn sinusoidal functions that are much more similar than the functions learned by their narrower counterparts (Fig. 4). We have analogous plots for all of the other widths and ones that visualize the variance similar to how it is commonly visualized for Gaussian processes in Appendix B.5.

4. Variance and Depth

In this section, we study the effect of depth on bias and variance by fixing width and varying depth. Nearly all studies of the trend of test error with increasing network size focus on width (and not depth). This is at least partially because there are pathological problems that cause deeper networks to experience higher test error than their shallower counterparts (Glorot & Bengio, 2010; He et al., 2016; Balduzzi et al., 2017). This indicates that there are some important confounding factors to control for when varying depth. The best control that we found is to use an initialization that achieves *dynamical isometry*, the condition that all of the singular values of the input-output Jacobian are 1 at initialization (Saxe et al., 2014; Pennington et al., 2017), as it allows us to observe decreasing bias with depth (Fig. 5a). See Appendix C.1 for more discussion on this.

4.1. Total Variance Experiments

We train fully connected networks up to 200 layers deep and observe slowly increasing variance with depth (Fig. 5a). The experimental protocol is similar to what it was in Section 3, with a few differences: All networks have width 100 and achieve 0 training error. We train them to the same loss value of 5e-5 to control for differences in training loss. This value was chosen carefully by observing when training error had been 0 for a long time. Like in Section 3.3, we tune the step size for each depth to ensure

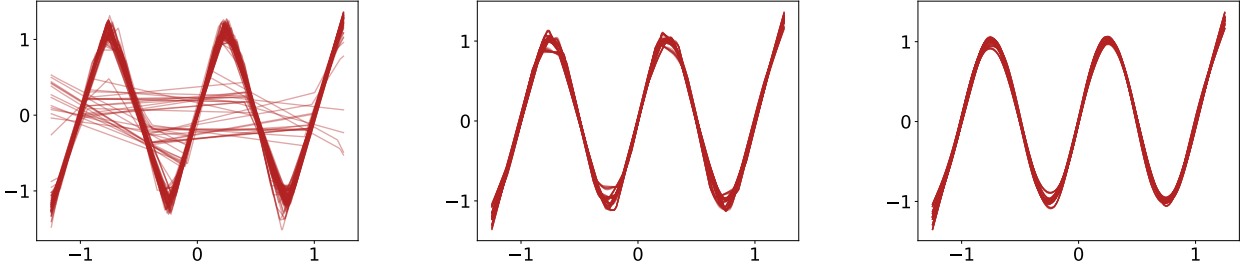
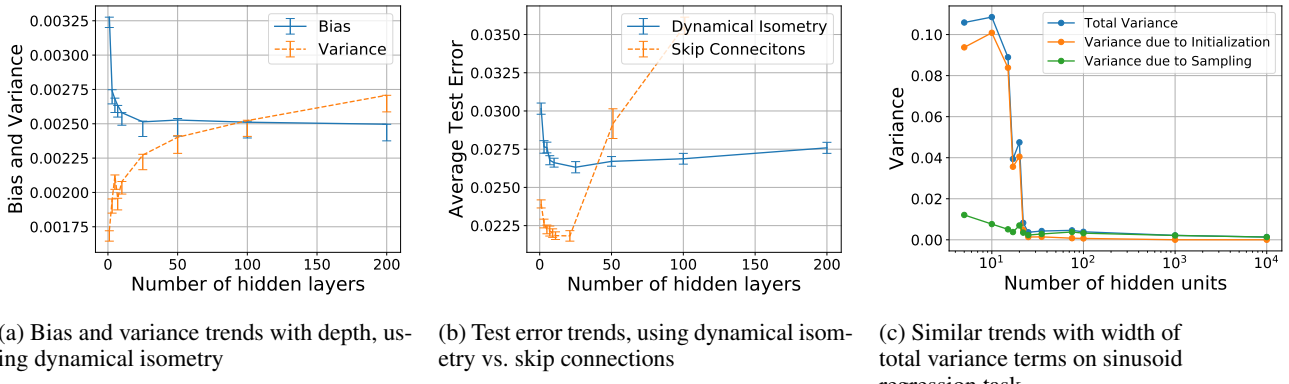


Figure 4: Visualization of the 100 different learned functions of single hidden layer neural networks of widths 15, 1000, and 10000 (from left to right) on the task of learning a sinusoid. The learned functions are increasingly similar with width, not increasingly different. More in Appendix B.5.



decreasing bias with depth. The 3 kinds of different networks we train are vanilla fully connected, fully connected with skip connections, and fully connected with dynamical isometry initialization. We only show the experiment with dynamical isometry in the main paper, but the other two are in Appendix C.2 and Appendix C.3.

We settle on fully connected networks without skip connections, initialized using the initialization Pennington et al. (2017) recommend to achieve dynamical isometry. This is the best experimental protocol of the three we tried because it appears to largely mitigate the pathological problems that cause deeper networks to have higher bias and test error. We compare the test accuracy of skip connections to that of dynamical isometry in Fig. 5b³ to see that while the test accuracy of skip connections varies by over 1% from depth 25 to 100, the corresponding error bars for the dynamical isometry test errors overlap (although test error does increase by about 0.1% from depth 25 to 200). In addition to this near lack of dependence of test error on depth, the dynamical isometry setup is the only one we found to

³Note that the best dynamical isometry network achieves test set accuracy of about 0.4% worse than the best skip connection network due to the fact that dynamical isometry is not possible with ReLU activations, so Tanh is used (Pennington et al., 2017).

achieve monotonically decreasing bias with depth (Fig. 5a, Appendix C). This bias trend is why we view this experiment as having controlled for confounding factors sufficiently well.

4.2. Decoupling Variance due to Sampling from Variance due to Initialization

To get a more fine-grain look at the effect of depth on variance, we estimate the terms of the law of total variance in Fig. 2, just as we did for width. Surprisingly, *variance due to sampling is roughly constant*. Variance due to initialization increases with depth.

We view the increase in variance due to initialization that we observe as consistent with the conventional wisdom that Arora et al. (2018) summarizes: “Conventional wisdom in deep learning states that increasing depth improves expressiveness but complicates optimization.” While Arora et al. (2018) focus on speed of training, the variance we measure in Fig. 2 is about the diversity of different minima. Increasing depth seems to lead to different initial starting points optimizing to increasingly different functions, as evaluated on the *test set*. Li et al. (2017, Figure 5) provide visualizations that suggest that increasing depth leads to increasingly “chaotic” loss landscapes, which would indicate in-

creasing variance on the training set.

5. Discussion and Theoretical Insights

Our empirical results demonstrate that in the practical setting, variance due to initialization decreases with network width while variance due to sampling remains constant. In Section 5.1, we discuss the simple case of linear models and point out that non-increasing variance can already be seen in the over-parameterized setting. In Section 5.2 we take inspiration from linear models to provide arguments for the behavior of variance in increasingly wide neural networks. In Section 5.3, we discuss the assumptions made in Section 5.2.

5.1. Insights from Linear Models

In this section, we review the classic result that the variance of a linear model grows with the number of parameters (Hastie et al., 2009, Section 7.3) and point out that variance behaves differently in the over-parameterized setting.

We consider least-squares linear regression in a standard setting which assumes a noisy linear mapping $y = \theta^T x + \epsilon$ between input feature vectors $x \in \mathbb{R}^N$ and real outputs, where ϵ denotes the noise random variable with $\mathbb{E}[\epsilon] = 0$ and $\text{Var}(\epsilon) = \sigma_\epsilon^2$. In this context, the over-parameterized setting is when the dimension N of the input space is larger than the number m of examples.

Let X denote the $m \times N$ design matrix whose i^{th} row is the training point x_i^T , let Y denote the corresponding labels, and let $\Sigma = X^T X$ denote the empirical covariance matrix. We consider the “fixed design” setting where X is fixed, so all of the randomness due to data sampling comes solely from ϵ . \mathcal{A} learns weights $\hat{\theta}$ from (X, Y) , either by a closed-form solution or by gradient descent, using a standard initialization $\theta_0 \sim \mathcal{N}(0, \frac{1}{N} I)$. The predictor makes a prediction on $x \sim \mathcal{D}$: $h(x) = \hat{\theta}^T x$. Then, the quantity we care about is $\mathbb{E}_x \text{Var}(h(x))$.

5.1.1. UNDER-PARAMETERIZED SETTING

The case where $N \leq m$ is standard: if X has maximal rank, Σ is invertible; the solution is independent of the initialization and given by $\hat{\theta} = \Sigma^{-1} X^T Y$. All of the variance is a result of randomness in the noise ϵ . For a fixed x ,

$$\text{Var}(h(x)) = \sigma_\epsilon^2 \text{Tr}(xx^T \Sigma^{-1}). \quad (5)$$

This grows with the number of parameters N . For example, taking the expected value over the empirical distribution, \hat{p} , of the sample, we recover that the variance grows with N :

$$\mathbb{E}_{x \sim \hat{p}} [\text{Var}(h(x))] = \frac{N}{m} \sigma_\epsilon^2. \quad (6)$$

We provide a reproduction of the proofs in Appendix D.1.

5.1.2. OVER-PARAMETERIZED SETTING

The over-parameterized case where $N > m$ is more interesting: even if X has maximal rank, Σ is not invertible. This leads to a subspace of solutions, but gradient descent yields a unique solution from updates that belong to the span of the training points x_i (row space of X) (Le-Cun et al., 1991), which is of dimension $r = \text{rank}(X) = \text{rank}(\Sigma)$. Correspondingly, no learning occurs in the null space of X , which is of dimension $N - r$. Therefore, gradient descent yields the solution that is closest to initialization: $\hat{\theta} = P_\perp(\theta_0) + \Sigma^+ X^T Y$, where P_\perp projects onto the null space of X and $+$ denotes the Moore-Penrose inverse.

The variance has two contributions: one due to initialization and one due to sampling (here, the noise ϵ), as in Eq. (4). These are made explicit in Proposition 1.

Proposition 1 (Variance in over-parameterized linear models). *Consider the over-parameterized setting where $N > m$. For a fixed x , the variance decomposition of Eq. (4) yields*

$$\text{Var}(h(x)) = \frac{1}{N} \|P_\perp(x)\|^2 + \sigma_\epsilon^2 \text{Tr}(xx^T \Sigma^+). \quad (7)$$

This does not grow with the number of parameters N . In fact, because Σ^{-1} is replaced with Σ^+ , the variance scales as the dimension of the data (i.e the rank of X), as opposed to the number of parameters. For example, taking the expected value over the empirical distribution, \hat{p} , of the sample, we obtain

$$\mathbb{E}_{x \sim \hat{p}_X} [\text{Var}(h(x))] = \frac{r}{m} \sigma_\epsilon^2, \quad (8)$$

where $r = \text{rank}(X)$. We provide the proofs for over-parameterized linear models in Appendix D.2.

5.2. A More General Result

We will illustrate our arguments in the following simplified setting, where \mathcal{M} , \mathcal{M}^\perp , and $d(N)$ are the more general analogs of $\text{rowspace}(X)$, $\text{nullspace}(X)$, and r (respectively):

Setting. Let N be the dimension of the parameter space. The prediction for a fixed example x , given by a trained network parameterized by θ depends on:

- (i) a subspace of the parameter space, $\mathcal{M} \in \mathbb{R}^N$ with relatively small dimension, $d(N)$, which depends only on the learning task.
- (ii) parameter components corresponding to directions orthogonal to \mathcal{M} . The orthogonal \mathcal{M}^\perp of \mathcal{M} has dimension, $N - d(N)$, and is essentially irrelevant to the learning task.

We can write the parameter vector as a sum of these two components $\theta = \theta_{\mathcal{M}} + \theta_{\mathcal{M}^\perp}$. We will further make the following assumptions.

Assumption 1 The optimization of the loss function is invariant with respect to $\theta_{\mathcal{M}^\perp}$.

Assumption 2 Regardless of initialization, the optimization method consistently yields a solution with the same $\theta_{\mathcal{M}}$ component, (i.e. the same vector when projected onto \mathcal{M}).

5.2.1. VARIANCE DUE TO INITIALIZATION

Given the above assumptions, the following result shows that the variance from initialization vanishes as we increase N . The full proof, which builds on concentration results for Gaussians (based on Levy’s lemma (Ledoux, 2001)), is given in [Appendix D](#).

Theorem 1 (Decay of variance due to initialization). *Consider the setting of Section 5.2 Let θ denote the parameters at the end of the learning process. Then, for a fixed data set and parameters initialized as $\theta_0 \sim \mathcal{N}(0, \frac{1}{N}I)$, the variance of the prediction satisfies the inequality,*

$$\text{Var}_{\theta_0}(h_\theta(x)) \leq C \frac{2L^2}{N} \quad (9)$$

where L is the Lipschitz constant of the prediction with respect to θ , and for some universal constant $C > 0$.

This result guarantees that the variance decreases to zero as N increases, provided the Lipschitz constant L grows more slowly than the square root of dimension, $L = o(\sqrt{N})$.

5.2.2. VARIANCE DUE TO SAMPLING

Under the above assumptions, the parameters at the end of learning take the form $\theta = \theta_{\mathcal{M}}^* + \theta_{0\mathcal{M}^\perp}$. For fixed initialization, the only source of variance of the prediction is the randomness of $\theta_{\mathcal{M}}^*$ on the learning manifold. The variance depends on the parameter dimensionality only through $\dim \mathcal{M} = d(N)$, and hence remains constant if $d(N)$ does (see [Li et al. \(2018\)](#)’s “intrinsic dimension”).

5.3. Discussion on Assumptions

We made strong assumptions, but there is some support for them in the literature. The existence of a subspace \mathcal{M}^\perp in which no learning occurs was also conjectured by [Advani & Saxe \(2017\)](#) and shown to hold in linear neural networks under a simplifying assumption that decouples the dynamics of the weights in different layers. [Li et al. \(2018\)](#) empirically showed the existence of a critical number $d(N) = d$ of relevant parameters for a given learning task, independent of the size of the model. [Sagun et al. \(2017\)](#) showed that the spectrum of the Hessian for over-parameterized networks splits into (i) a bulk centered near zero and (ii) a small number of large eigenvalues; and [Gur-Ari et al. \(2018\)](#) recently gave evidence that the small

subspace spanned by the Hessian’s top eigenvectors is preserved over long periods of training. These results suggest that learning occurs mainly in a small number of directions.

The mismatch between the outcome of our theoretical analysis and the observed trend of variance due to initialization with depth suggests that our assumptions are increasingly inaccurate with depth. For some intuition about why this may be the case, consider the dependence of gradients with respect to subsets of hidden units, as these gradients are related to **Assumption 1**: the invariance of the optimization process to $\theta_{\mathcal{M}^\perp}$. Gradients of hidden units in the same layer (related to width) do not directly depend on each other; rather, only optimization induces dependencies between them via the loss function. In sharp contrast, hidden units in different layers (related to depth) are functions of their preceding layers, and similarly, the gradients with respect to earlier layers are *functionally dependent* on the gradients with respect to later layers. This hints at more complex optimization interactions between parameters when increasing depth.

6. Conclusion and Future Work

By revisiting the bias-variance decomposition and using a finer-grain method to empirically study variance, we find interesting phenomena. First, we provide evidence against [Geman et al. \(1992\)](#)’s claim that “the price to pay for achieving low bias is high variance,” finding that *both* bias and variance decrease with width. Second, variance due to sampling (analog of regular variance in simple settings) does not appear to be dependent on width or, surprisingly, depth. Third, variance due to initialization is roughly consistent with the optimization literature, as we observe the test set analog of the current conventional wisdom for both width and depth. Finally, by taking inspiration from linear models, we perform a theoretical analysis of the variance that is consistent with our empirical observations for increasing width.

We view future work that uses the bias-variance lens as promising. For example, a probabilistic notion of effective capacity of a model is natural when studying generalization through this lens ([Appendix A](#)). We did not study how bias and variance change over the course of training; that would make an interesting direction for future work. Additionally, it may be fruitful to apply the bias-variance lens to other network architectures, such as convolutional networks and recurrent networks. More theoretical work is also needed to achieve a full understanding of the behaviour of variance in deep models. Variance is analytically different from generalization error in that the definition of variance does not involve the labels at all. We view the bias-variance lens as a useful tool for studying generalization in deep learning and hope to encourage more work in this direction.

Acknowledgments

We thank Yoshua Bengio, Lechao Xiao, Aaron Courville, Sharan Vaswani, Roman Novak, Xavier Bouthillier, Stanislaw Jastrzebski, Gaetan Marceau Caron, Rémi Le Priol, Guillaume Lajoie, and Joseph Cohen for helpful discussions. Additionally, we thank SigOpt for access to their professional hyperparameter tuning services. This research was partially supported by the NSERC Discovery Grant RGPIN-2017-06936, by a Google Focused Research Award, and by the FRQNT nouveaux chercheurs program, 2019-NC-257943. We thank NVIDIA for donating a DGX-1 computer used in this work.

References

Advani, M. S. and Saxe, A. M. High-dimensional dynamics of generalization error in neural networks. *CoRR*, abs/1710.03667, 2017.

Arora, S., Cohen, N., and Hazan, E. On the optimization of deep networks: Implicit acceleration by overparameterization. In Dy, J. and Krause, A. (eds.), *Proceedings of the 35th International Conference on Machine Learning*, volume 80 of *Proceedings of Machine Learning Research*, pp. 244–253, Stockholm, Sweden, 10–15 Jul 2018. PMLR.

Arpit, D., Jastrzebski, S., Ballas, N., Krueger, D., Bengio, E., Kanwal, M. S., Maharaj, T., Fischer, A., Courville, A., Bengio, Y., and Lacoste-Julien, S. A closer look at memorization in deep networks. *ICML 2017*, 70:233–242, 06–11 Aug 2017.

Balduzzi, D., Frean, M., Leary, L., Lewis, J. P., Ma, K. W.-D., and McWilliams, B. The shattered gradients problem: If resnets are the answer, then what is the question? In Precup, D. and Teh, Y. W. (eds.), *Proceedings of the 34th International Conference on Machine Learning*, volume 70 of *Proceedings of Machine Learning Research*, pp. 342–350, International Convention Centre, Sydney, Australia, 06–11 Aug 2017. PMLR.

Belkin, M., Hsu, D., Ma, S., and Mandal, S. Reconciling modern machine learning and the bias-variance tradeoff. *arXiv e-prints*, art. arXiv:1812.11118, December 2018.

Bengio, Y., Simard, P., and Frasconi, P. Learning long-term dependencies with gradient descent is difficult. *IEEE Transactions on Neural Networks*, 5(2):157–166, March 1994.

Bishop, C. M. *Pattern Recognition and Machine Learning (Information Science and Statistics)*. Springer-Verlag, Berlin, Heidelberg, 2006.

Bousquet, O. and Elisseeff, A. Stability and generalization. *Journal of Machine Learning Research*, 2:499–526, March 2002.

Canziani, A., Paszke, A., and Culurciello, E. An analysis of deep neural network models for practical applications. *CoRR*, abs/1605.07678, 2016.

Domingos, P. A unified bias-variance decomposition and its applications. In *In Proc. 17th International Conf. on Machine Learning*, pp. 231–238. Morgan Kaufmann, 2000.

Du, S. and Lee, J. On the power of over-parametrization in neural networks with quadratic activation. In Dy, J. and Krause, A. (eds.), *Proceedings of the 35th International Conference on Machine Learning*, volume 80 of *Proceedings of Machine Learning Research*, pp. 1329–1338, Stockholm, Sweden, 10–15 Jul 2018. PMLR.

Du, S., Zhai, X., Poczos, B., and Singh, A. Gradient descent provably optimizes over-parameterized neural networks. volume abs/1810.02054, 2019.

Dziugaite, G. K. and Roy, D. M. Computing nonvacuous generalization bounds for deep (stochastic) neural networks with many more parameters than training data. In *Proceedings of the Thirty-Third Conference on Uncertainty in Artificial Intelligence, UAI 2017, Sydney, Australia, August 11–15, 2017*, 2017.

Efron, B. Bootstrap methods: Another look at the jackknife. *Ann. Statist.*, 7(1):1–26, 01 1979.

EliteDataScience. Wtf is the bias-variance tradeoff? (info-graphic), May 2018.

Fortmann-Roe, S. Understanding the bias-variance tradeoff, June 2012.

Geman, S., Bienenstock, E., and Doursat, R. Neural networks and the bias/variance dilemma. *Neural Computation*, 4(1):1–58, 1992.

Glorot, X. and Bengio, Y. Understanding the difficulty of training deep feedforward neural networks. In Teh, Y. W. and Titterington, M. (eds.), *Proceedings of the Thirteenth International Conference on Artificial Intelligence and Statistics*, volume 9 of *Proceedings of Machine Learning Research*, pp. 249–256, Chia Laguna Resort, Sardinia, Italy, 13–15 May 2010. PMLR.

Gonzalez, J. E. Linear regression and the bias variance tradeoff, 2016. lecture notes.

Gunasekar, S., Lee, J., Soudry, D., and Srebro, N. Characterizing implicit bias in terms of optimization geometry. In Dy, J. and Krause, A. (eds.), *Proceedings of*

the 35th International Conference on Machine Learning, volume 80 of *Proceedings of Machine Learning Research*, pp. 1832–1841, Stockholm, Sweden, 10–15 Jul 2018a. PMLR.

Gunasekar, S., Lee, J. D., Soudry, D., and Srebro, N. Implicit bias of gradient descent on linear convolutional networks. In Bengio, S., Wallach, H., Larochelle, H., Grauman, K., Cesa-Bianchi, N., and Garnett, R. (eds.), *Advances in Neural Information Processing Systems 31*, pp. 9482–9491. Curran Associates, Inc., 2018b.

Gur-Ari, G., Roberts, D. A., and Dyer, E. Gradient descent happens in a tiny subspace. *arXiv preprint arXiv: arXiv:1812.04754*, 2018.

Hastie, T., Tibshirani, R., and Friedman, J. *The elements of statistical learning: data mining, inference and prediction*. Springer, 2 edition, 2009.

He, K., Zhang, X., Ren, S., and Sun, J. Deep residual learning for image recognition. In *2016 IEEE Conference on Computer Vision and Pattern Recognition (CVPR)*, pp. 770–778, June 2016.

Hochreiter, S. Untersuchungen zu dynamischen neuronalen Netzen. Diploma thesis, Institut für Informatik, Lehrstuhl Prof. Brauer, Technische Universität München, 1991.

Ioffe, S. and Szegedy, C. Batch normalization: Accelerating deep network training by reducing internal covariate shift. In Bach, F. and Blei, D. (eds.), *Proceedings of the 32nd International Conference on Machine Learning*, volume 37 of *Proceedings of Machine Learning Research*, pp. 448–456, Lille, France, 07–09 Jul 2015. PMLR.

James, G. M. Variance and bias for general loss functions. In *Machine Learning*, pp. 115–135, 2003.

Keskar, N. S., Mudigere, D., Nocedal, J., Smelyanskiy, M., and Tang, P. T. P. On large-batch training for deep learning: Generalization gap and sharp minima. In *International Conference on Learning Representations*, 2017.

Kohavi, R. and Wolpert, D. Bias plus variance decomposition for zero-one loss functions. In *Proceedings of the Thirteenth International Conference on International Conference on Machine Learning*, ICML’96, pp. 275–283, San Francisco, CA, USA, 1996. Morgan Kaufmann Publishers Inc.

Kuzborskij, I. and Lampert, C. Data-dependent stability of stochastic gradient descent. In Dy, J. and Krause, A. (eds.), *Proceedings of the 35th International Conference on Machine Learning*, volume 80 of *Proceedings of Machine Learning Research*, pp. 2815–2824, Stockholm, Sweden, 10–15 Jul 2018. PMLR.

LeCun, Y., Kanter, I., and Solla, S. Eigenvalues of covariance matrices: Application to neural-network learning. *Physical Review Letters*, 66:2396–2399, 05 1991.

Ledoux, M. *The Concentration of Measure Phenomenon*. Mathematical surveys and monographs. American Mathematical Society, 2001.

Li, C., Farkhoor, H., Liu, R., and Yosinski, J. Measuring the intrinsic dimension of objective landscapes. *ICLR 2018*, 2018.

Li, H., Xu, Z., Taylor, G., and Goldstein, T. Visualizing the loss landscape of neural nets. *CoRR*, abs/1712.09913, 2017.

Livni, R., Shalev-Shwartz, S., and Shamir, O. On the computational efficiency of training neural networks. In Ghahramani, Z., Welling, M., Cortes, C., Lawrence, N. D., and Weinberger, K. Q. (eds.), *Advances in Neural Information Processing Systems 27*, pp. 855–863. Curran Associates, Inc., 2014.

Neyshabur, B. Implicit regularization in deep learning. *arXiv preprint arXiv:1709.01953*, 2017.

Neyshabur, B., Tomioka, R., and Srebro, N. In search of the real inductive bias: On the role of implicit regularization in deep learning. *International Conference on Learning Representations workshop track*, 2015.

Neyshabur, B., Li, Z., Bhojanapalli, S., LeCun, Y., and Srebro, N. The role of over-parametrization in generalization of neural networks. In *International Conference on Learning Representations*, 2019.

Novak, R., Bahri, Y., Abolafia, D. A., Pennington, J., and Sohl-Dickstein, J. Sensitivity and generalization in neural networks: an empirical study. In *International Conference on Learning Representations*, 2018.

Pennington, J., Schoenholz, S., and Ganguli, S. Resurrecting the sigmoid in deep learning through dynamical isometry: theory and practice. In Guyon, I., Luxburg, U. V., Bengio, S., Wallach, H., Fergus, R., Vishwanathan, S., and Garnett, R. (eds.), *Advances in Neural Information Processing Systems 30*, pp. 4785–4795. Curran Associates, Inc., 2017.

Sagun, L., Evci, U., Guney, V. U., Dauphin, Y., and Bottou, L. Empirical analysis of the hessian of over-parametrized neural networks. 2017.

Saxe, A. M., McClelland, J. L., and Ganguli, S. Exact solutions to the nonlinear dynamics of learning in deep linear neural network. In *In International Conference on Learning Representations*, 2014.

Schoenholz, S. S., Gilmer, J., Ganguli, S., and Sohl-Dickstein, J. Deep information propagation. *ICLR 2017*, 2017.

Smith, S. L., Kindermans, P.-J., and Le, Q. V. Don't decay the learning rate, increase the batch size. In *International Conference on Learning Representations*, 2018.

Soltanolkotabi, M., Javanmard, A., and Lee, J. D. Theoretical insights into the optimization landscape of over-parameterized shallow neural networks. *CoRR*, abs/1707.04926, 2017.

Soudry, D., Hoffer, E., and Srebro, N. The implicit bias of gradient descent on separable data. In *International Conference on Learning Representations*, 2018.

Spigler, S., Geiger, M., d'Ascoli, S., Sagun, L., Biroli, G., and Wyart, M. A jamming transition from under- to over-parametrization affects loss landscape and generalization. *CoRR*, abs/1810.09665, 2018.

Vapnik, V. N. An overview of statistical learning theory. *Trans. Neur. Netw.*, 10(5):988–999, September 1999.

Xiao, L., Bahri, Y., Sohl-Dickstein, J., Schoenholz, S., and Pennington, J. Dynamical isometry and a mean field theory of CNNs: How to train 10,000-layer vanilla convolutional neural networks. In Dy, J. and Krause, A. (eds.), *Proceedings of the 35th International Conference on Machine Learning*, volume 80 of *Proceedings of Machine Learning Research*, pp. 5393–5402, Stockholm, Sweden, 10–15 Jul 2018. PMLR.

Zhang, C., Bengio, S., Hardt, M., Recht, B., and Vinyals, O. Understanding deep learning requires rethinking generalization. *ICLR 2017*, 2017.

Zhang, C., Liao, Q., Rakhlin, A., Miranda, B., Golowich, N., and Poggio, T. A. Theory of deep learning iib: Optimization properties of SGD. *CoRR*, abs/1801.02254, 2018.

Appendices

A. Probabilistic notion of effective capacity

The problem with classical complexity measures is that they do not take into account optimization and have no notion of what will actually be learned. Arpit et al. (2017, Section 1) define a notion of an *effective* hypothesis class to take into account what functions are possible to be learned by the learning algorithm.

However, this still has the problem of not taking into account what hypotheses are *likely* to be learned. To take into account the probabilistic nature of learning, we define the ϵ -*hypothesis class* for a data distribution \mathcal{D} and learning algorithm \mathcal{A} , that contains the hypotheses which are at least ϵ -likely for some $\epsilon > 0$:

$$\mathcal{H}_{\mathcal{D}}(\mathcal{A}) = \{h : p(h(\mathcal{A}, S)) \geq \epsilon\}, \quad (10)$$

where S is a training set drawn from \mathcal{D}^m , $h(\mathcal{A}, S)$ is a random variable drawn from the distribution over learned functions induced by \mathcal{D} and the randomness in \mathcal{A} ; p is the corresponding density. Thinking about a model's ϵ -hypothesis class can lead to drastically different intuitions for the complexity of a model and its variance (Fig. 6). This is at the core of the intuition for why the traditional view of bias-variance as a tradeoff does not hold in all cases.

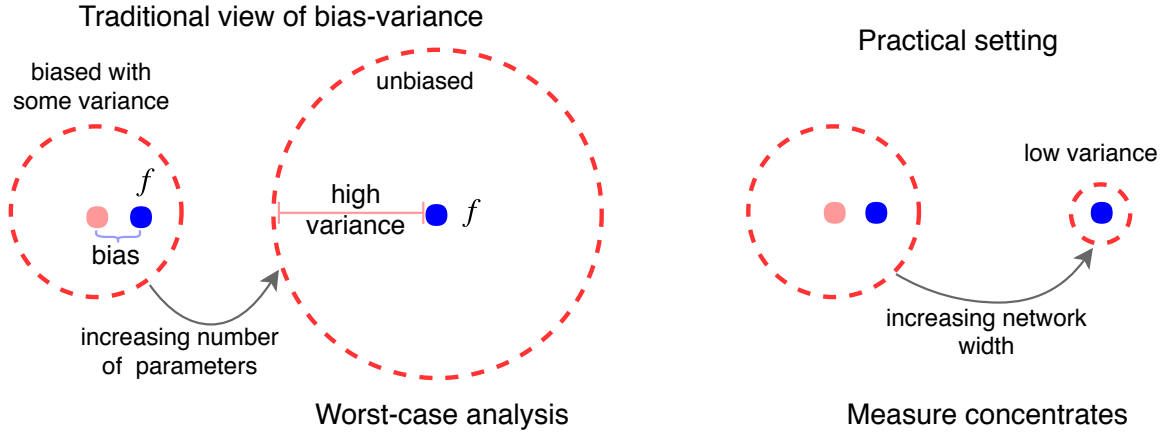


Figure 6: The dotted red circle depicts a cartoon version of the ϵ -hypothesis class of the learner. The left side reflects common intuition, as informed by the bias-variance tradeoff and worst-case analysis from statistical learning theory. The right side reflects our view that variance can decrease with network width.

B. Width and variance: additional empirical results and discussion

B.1. CIFAR10

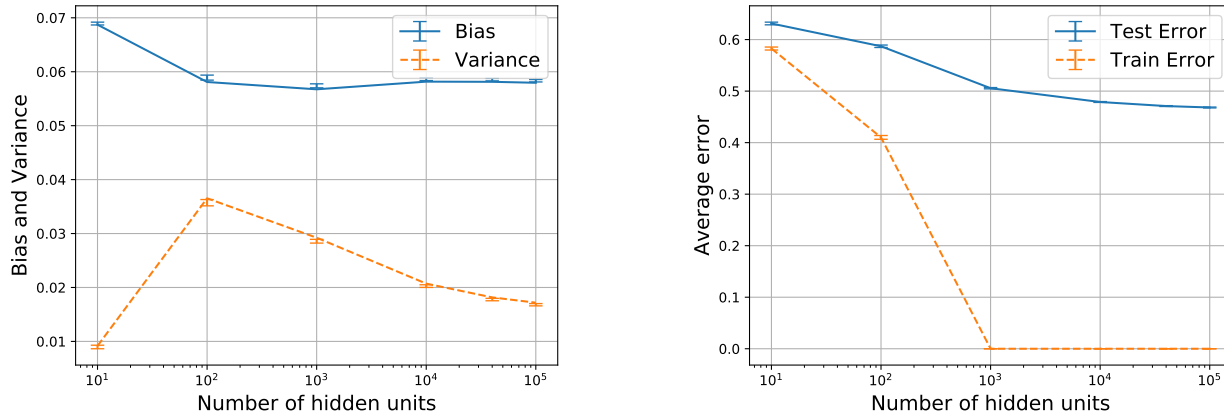


Figure 7: Bias-variance plot (left) and corresponding train and test error (right) for CIFAR10 after training for 150 epochs with step size 0.005 for all networks.

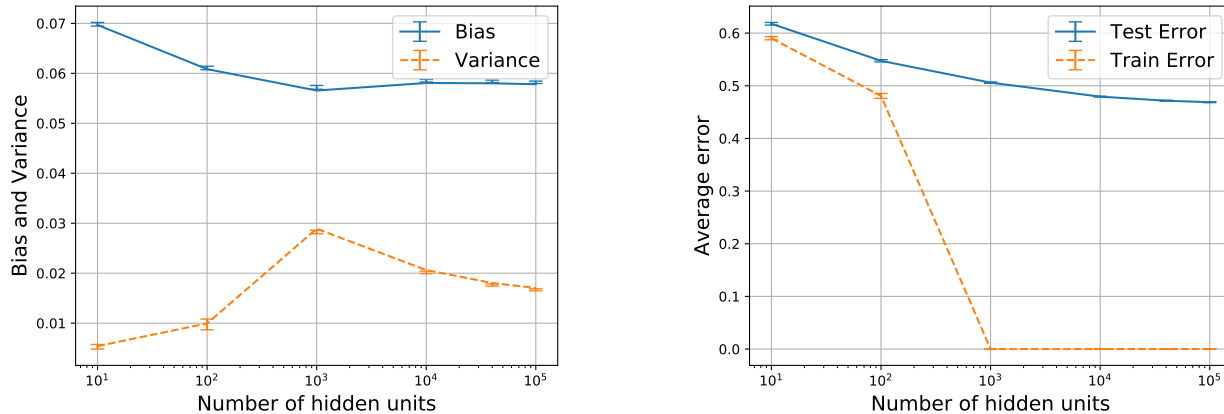
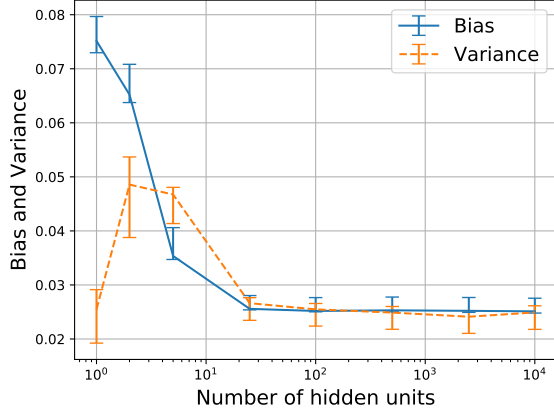
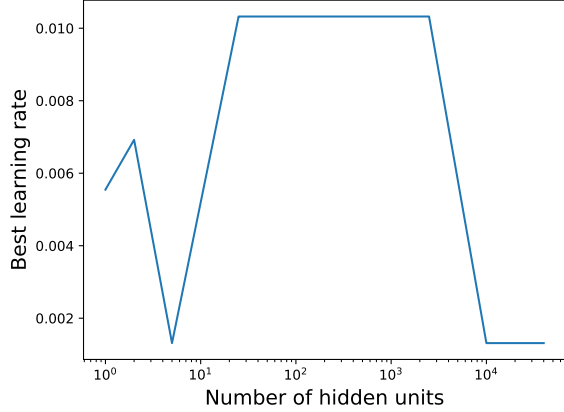


Figure 8: Bias-variance plot (left) and corresponding train and test error (right) for CIFAR10 after training for using *early stopping* with step size 0.005 for all networks.

B.2. Tuned learning rates for SGD


(a) Variance decreases with width, even in the small data setting (SGD). This figure is in the main paper, but we include it here to compare with the corresponding step sizes used.



(b) Corresponding optimal learning rates found, by random search, and used.

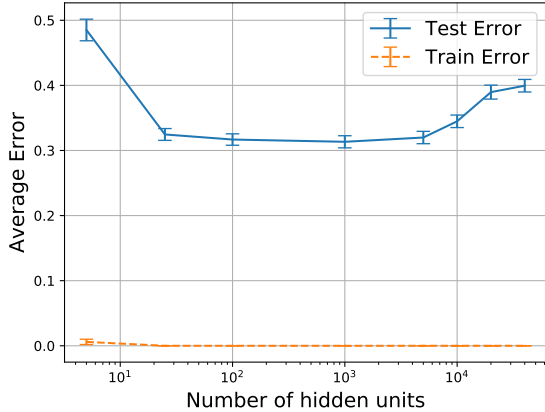
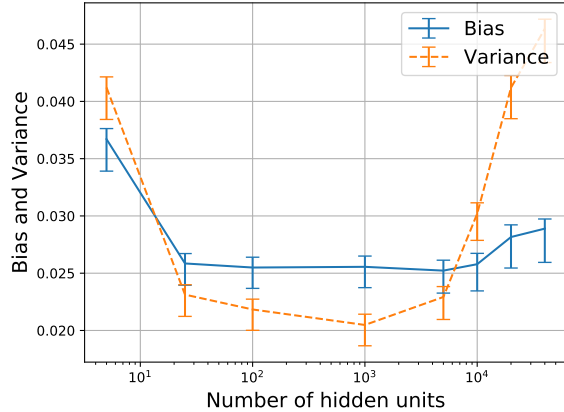
B.3. Fixed learning rate results for small data MNIST


Figure 10: Variance on small data with a fixed learning rate of 0.01 for all networks.

Note that the U curve shown in Fig. 10 when we do not tune the step size is explained by the fact that the constant step chosen is a “good” step size for some networks and “bad” for others. Results from Keskar et al. (2017) and Smith et al. (2018) show that a step size that corresponds well to the noise structure in SGD is important for achieving good test set accuracy. Because our networks are different sizes, their stochastic optimization process will have a different landscape and noise structure. By tuning the step size, we are making the experimental design choice to keep *optimality of step size* constant across networks, rather than keeping step size constant across networks. To us, choosing this control makes much more sense than choosing to control for step size.

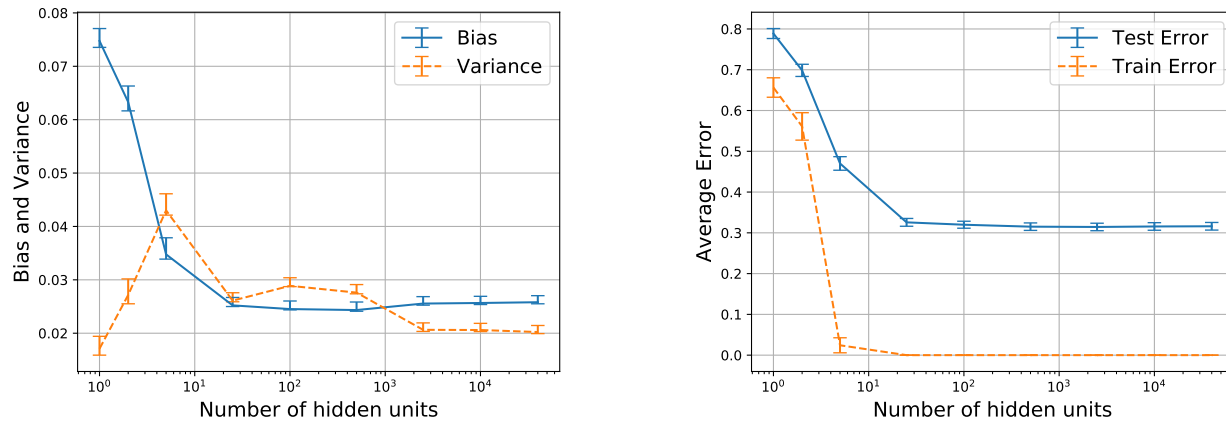
B.4. Other optimizers for width experiment on small data mnist


Figure 11: Variance decreases with width in the small data setting, even when using batch gradient descent.

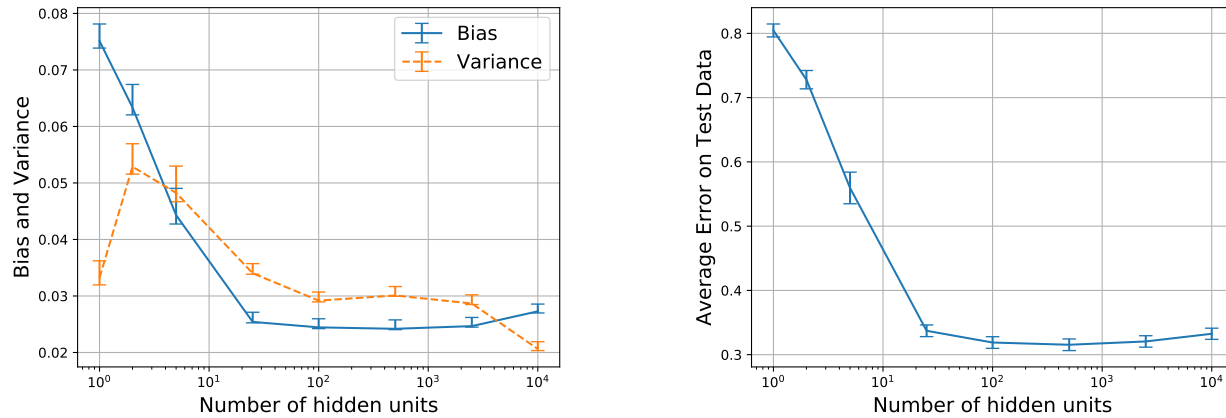
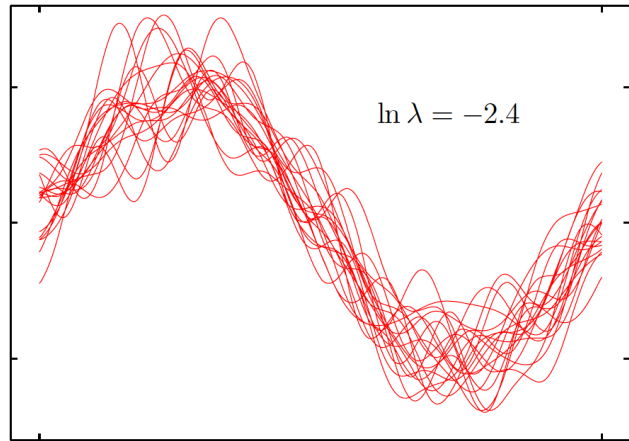
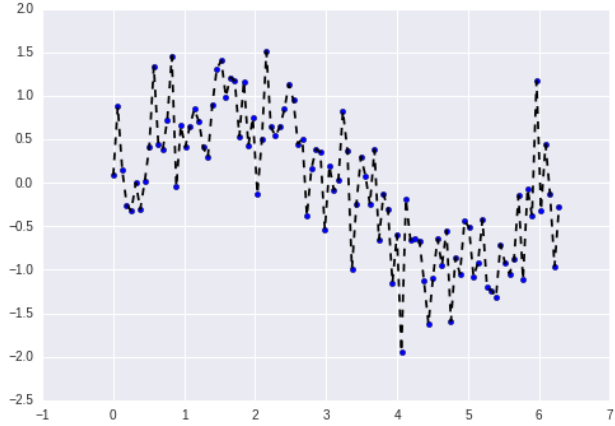


Figure 12: Variance decreases with width in the small data setting, even when using a strong optimizer, such as PyTorch's LBFGS, as the optimizer.

B.5. Sinusoid regression experiments



(a) Example of the many different functions learned by a high variance learner (Bishop, 2006, Section 3.2)



(b) Caricature of a single function learned by a high variance learner (EliteDataScience, 2018)

Figure 13: Caricature examples of high variance learners on sinusoid task. Below, we find that this does not happen with increasingly wide neural networks (Fig. 15 and Fig. 16).

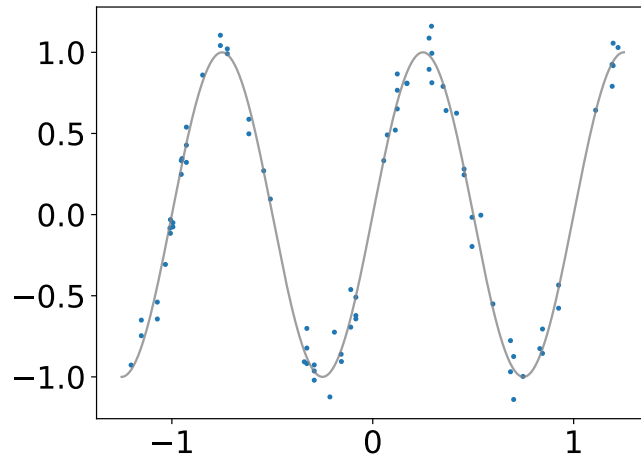


Figure 14: Target function of the noisy sinusoid regression task (in gray) and an example of a training set (80 data points) sampled from the noisy distribution.

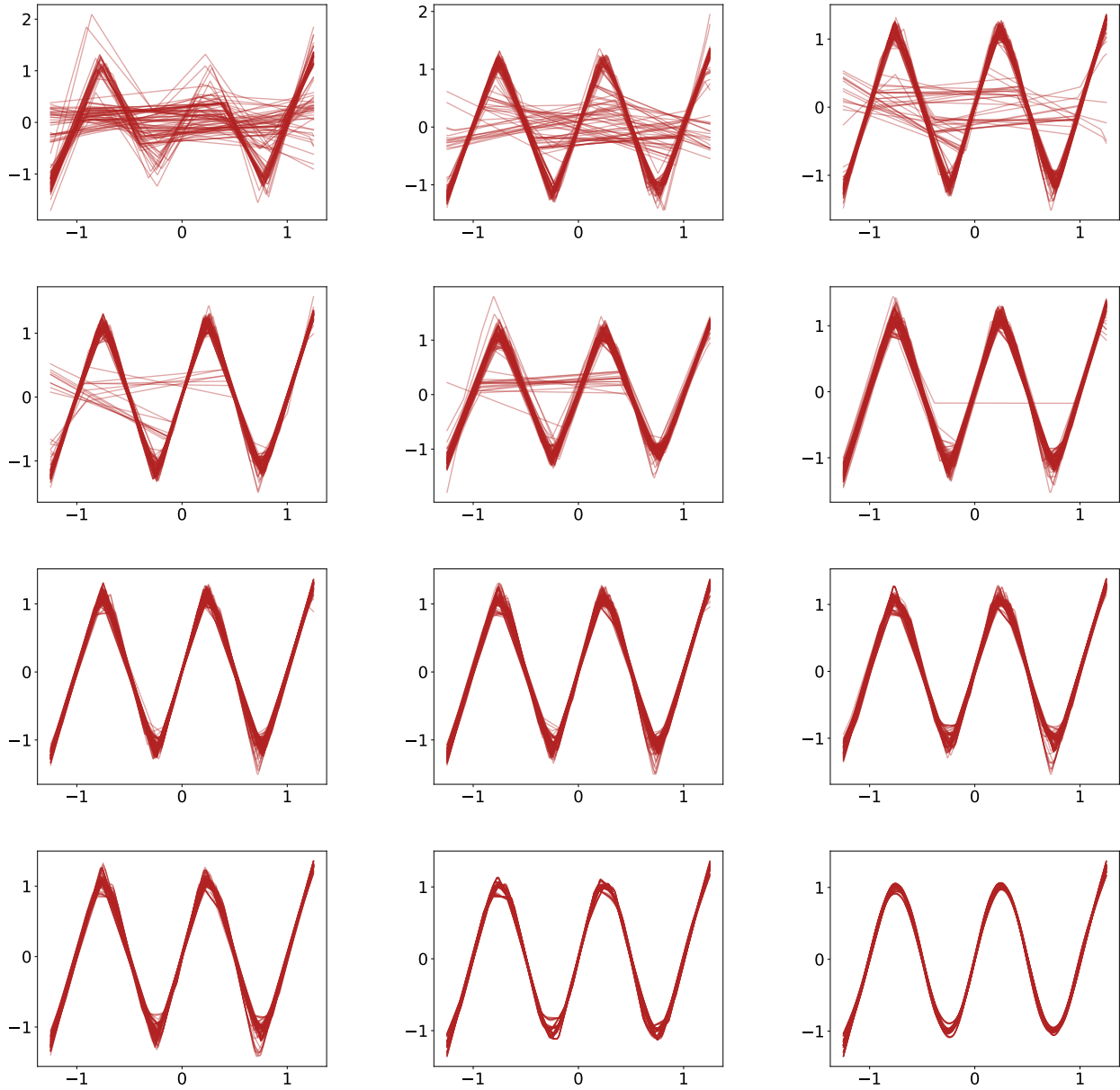


Figure 15: Visualization of 100 different functions learned by the different width neural networks. Darker color indicates higher density of different functions. Widths in increasing order from left to right and top to bottom: 5, 10, 15, 17, 20, 22, 25, 35, 75, 100, 1000, 10000. We do *not* observe the caricature from Fig. 13 as width is increased.

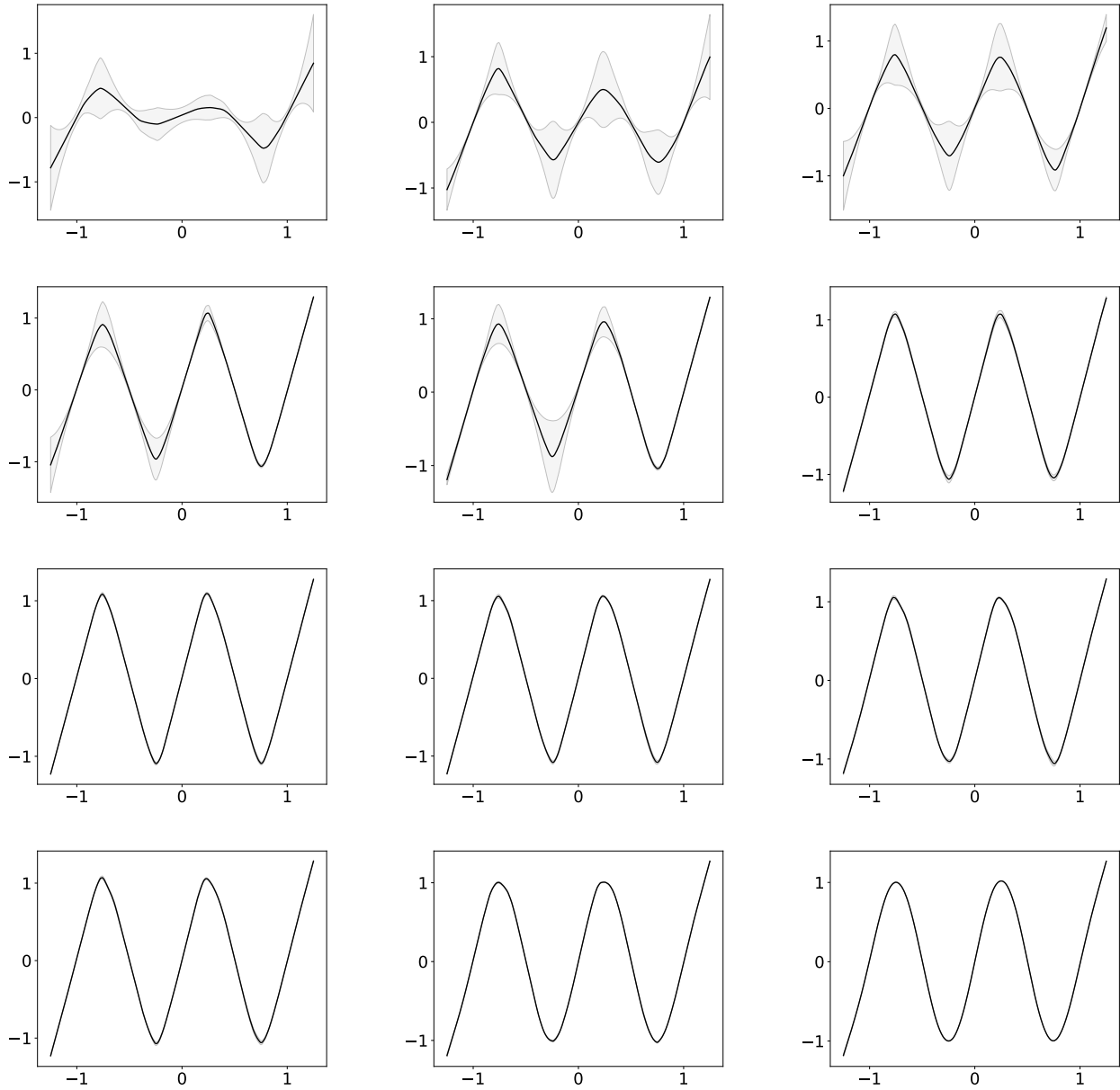


Figure 16: Visualization of the mean prediction and variance of the different width neural networks. Widths in increasing order from left to right and top to bottom: 5, 10, 15, 17, 20, 22, 25, 35, 75, 100, 1000, 10000.

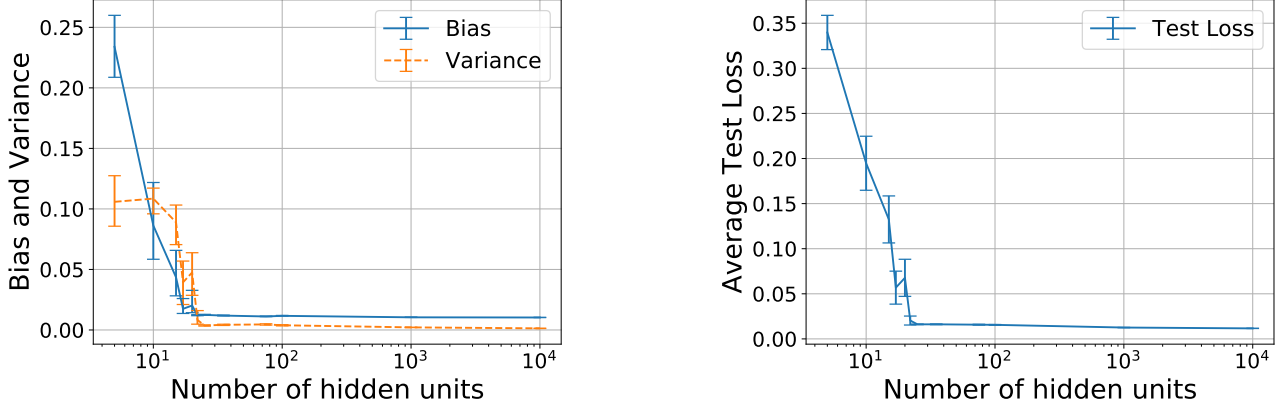


Figure 17: We observe the same trends of bias and total variance in the sinusoid regression setting. The figure on the left is in the main paper, while the figure on the right is support.

C. Depth and variance: additional empirical results and discussion

C.1. Discussion on need for careful experimental design

Depth is an important component of deep learning. We study its effect on bias and variance by fixing width and varying depth. However, there are pathological problems associated with training very deep networks such as vanishing/exploding gradient (Hochreiter, 1991; Bengio et al., 1994; Glorot & Bengio, 2010), signal not being able to propagate through the network (Schoenholz et al., 2017), and gradients resembling white noise (Baldazzi et al., 2017). He et al. (2016) pointed out that very deep networks experience high test set error and argued it was due to high training set loss. However, while skip connections (He et al., 2016), better initialization (Glorot & Bengio, 2010), and batch normalization (Ioffe & Szegedy, 2015) have largely served to facilitate low training loss in very deep networks, the problem of high *test set* error still remains.

The current best practices for achieving low test error in very deep networks arose out of trying to solve the above problems in training. An initial step was to ensure the mean squared singular value of the input-output Jacobian, at initialization, is close to 1 (Glorot & Bengio, 2010). More recently, there has been work on a stronger condition known as *dynamical isometry*, where *all* singular values remain close to 1 (Saxe et al., 2014; Pennington et al., 2017). Pennington et al. (2017) also empirically found that dynamical isometry helped achieve low test set error. Furthermore, Xiao et al. (2018, Figure 1) found evidence that test set performance did not degrade with depth when they lifted dynamical isometry to CNNs. This is why we settled on dynamical isometry as the best known practice to control for as many confounding factors as possible.

We first ran experiments with vanilla full connected networks (Fig. 18). These have clear training issues where networks of depth more than 20 take very long to train to the target training loss of 5e-5. The bias curve is not even monotonically decreasing. Clearly, there are important confounding factors not controlled for in this simple setting. Still, note that variance increases roughly linearly with depth.

We then study fully connected networks with skip connections between every 2 layers (Fig. 19). While this allows us to train deeper networks than without skip connections, many of the same issues persist (e.g. bias still not monotonically decreasing). The bias, variance, and test error curves are all checkmark-shaped.

C.2. Vanilla fully connected depth experiments

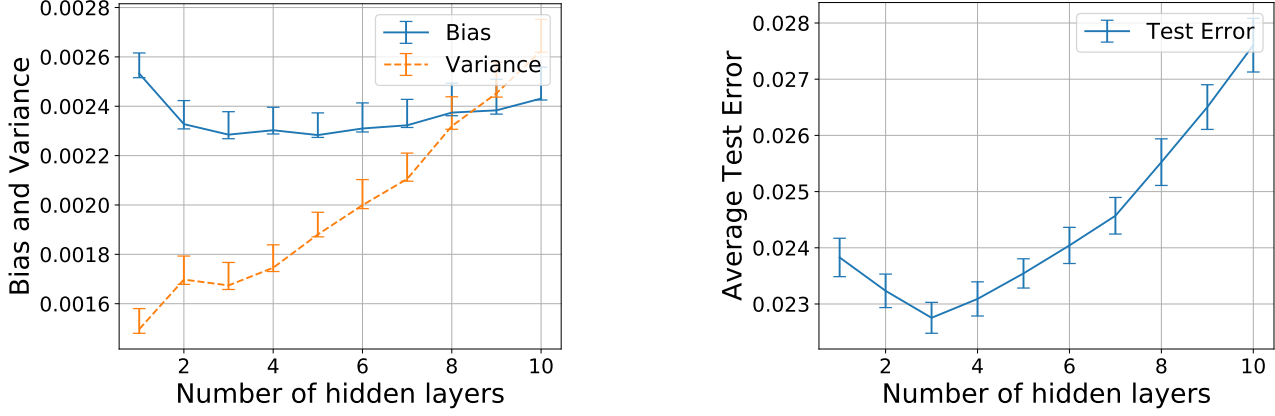


Figure 18: Test error quickly degrades in fairly shallow fully connected networks, and bias does not even monotonically decrease with depth. However, this is the first indication that variance might *increase* with depth. All networks have training error 0 and are trained to the same training loss of 5e-5.

C.3. Skip connections depth experiments

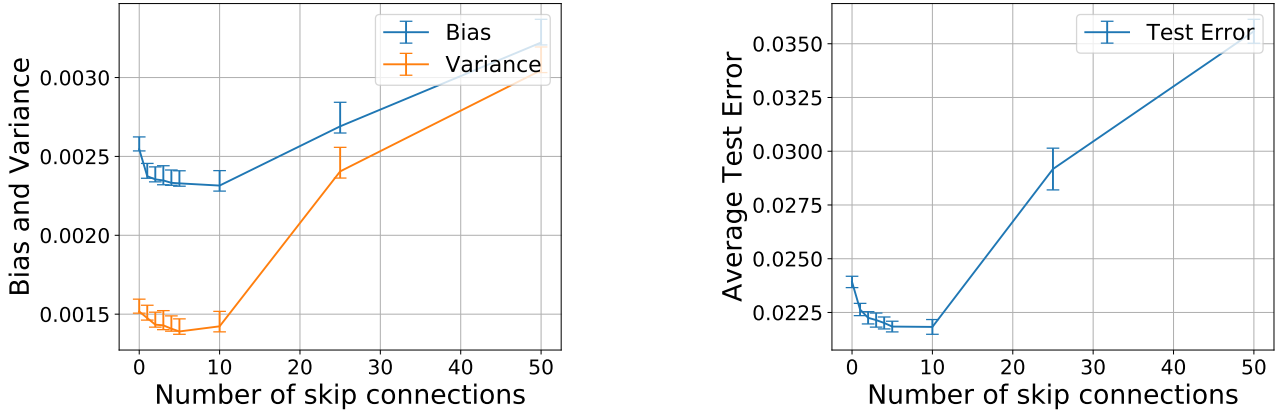


Figure 19: While the addition of skip connections (between every other layer) might push the bottom of the U curve in test error out to 10 skip connections (21 layers), which is further than 3 layers, which is what was seen without skip connections, test error still degrades noticeably in greater depths. Additionally, bias still does not even monotonically decrease with depth. While skip connections appear to have helped control for the factors we want to control, they were not completely satisfying. All networks have training error 0 and are trained to the same training loss of 5e-5.

C.4. Dynamical isometry depth experiments

The figures in this section are included in the main paper, but they are included here for comparison to the above and for completeness.

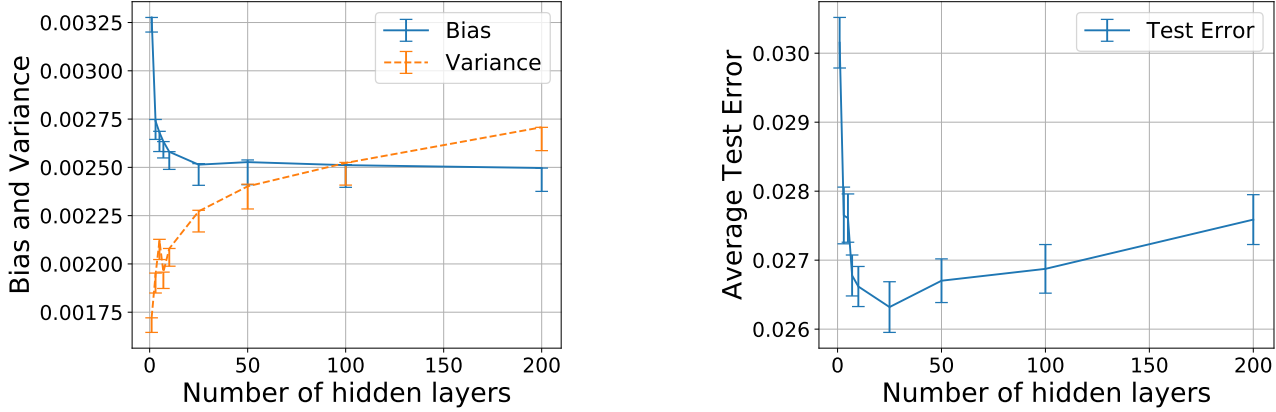


Figure 20: Additionally, dynamical isometry seems to cause bias to decrease monotonically with depth. While skip connections appear to have helped control for the factors we want to control, they were not completely satisfying. All networks have training error 0 and are trained to the same training loss of 5e-5.

D. Some Proofs

D.1. Proof of Classic Result for Variance of Linear Model

Here, we reproduce the classic result that variance grows with the number of parameters in a linear model. This result can be found in [Hastie et al. \(2009\)](#)'s book, and a similar proof can be found in [Gonzalez \(2016\)](#)'s lecture slides.

Proof. For a fixed x , we have $h(x) = x^T \hat{\theta}$. Taking $\hat{\theta} = \Sigma^{-1} X^T Y$ to be the gradient descent solution, and using $Y = X\theta + \epsilon$, we obtain:

$$h(x) = x^T \Sigma^{-1} X^T (X\theta + \epsilon) = x^T \theta + x^T \Sigma^{-1} X^T \epsilon$$

Hence $\mathbb{E}_\epsilon[h(x)] = x^T \theta$, and the variance is,

$$\begin{aligned} \text{Var}_\epsilon(h(x)) &= \mathbb{E}_\epsilon[(h(x) - \mathbb{E}_\epsilon[h(x)])^2] \\ &= \mathbb{E}_\epsilon[(x^T \theta + x^T \Sigma^{-1} X^T \epsilon - x^T \theta)^2] \\ &= \mathbb{E}_\epsilon[(x^T \Sigma^{-1} X^T \epsilon)^2] \\ &= \mathbb{E}_\epsilon[(x^T \Sigma^{-1} X^T \epsilon)(x^T \Sigma^{-1} X^T \epsilon)^T] \\ &= \mathbb{E}_\epsilon[x^T \Sigma^{-1} X^T \epsilon \epsilon^T (x^T \Sigma^{-1} X^T)^T] \\ &= \sigma_\epsilon^2 x^T \Sigma^{-1} \Sigma \Sigma^{-1} x \\ &= \sigma_\epsilon^2 x^T \Sigma^{-1} \Sigma \Sigma^{-1} x \\ &= \sigma_\epsilon^2 x^T \Sigma^{-1} x \\ &= \sigma_\epsilon^2 \text{Tr}(x^T \Sigma^{-1} x) \\ &= \sigma_\epsilon^2 \text{Tr}(x x^T \Sigma^{-1}) \end{aligned}$$

Taking the expected value over the empirical distribution, \hat{p} , of the sample, we find an explicit increasing dependence on

N :

$$\begin{aligned}
 \mathbb{E}_{x \sim \hat{p}}[\text{Var}_\epsilon(h(x))] &= \mathbb{E}_{x \sim \hat{p}}[\sigma_\epsilon^2 \text{Tr}(xx^T \Sigma^{-1})] \\
 &= \sigma_\epsilon^2 \text{Tr}(\mathbb{E}_{x \sim \hat{p}}[xx^T] \Sigma^{-1}) \\
 &= \sigma_\epsilon^2 \text{Tr}\left(\frac{1}{m} \Sigma \Sigma^{-1}\right) \\
 &= \sigma_\epsilon^2 \frac{1}{m} \text{Tr}(I_N) \\
 &= \sigma_\epsilon^2 \frac{N}{m}
 \end{aligned}$$

□

D.2. Proof of Result for Variance of Over-parameterized Linear Models

Here, we produce a variation on what was done in [Appendix D.1](#) to show that variance does not grow with the number of parameters in over-parameterized linear models. Recall that we are considering the setting where $N > m$, where N is the number of parameters and m is the number of training examples.

Proof. By the law of total variance,

$$\text{Var}(h(x)) = \mathbb{E}_\epsilon \text{Var}_{\theta_0}(h(x)) + \text{Var}_\epsilon(\mathbb{E}_{\theta_0}[h(x)])$$

Here have $h(x) = x^T \hat{\theta}$, where $\hat{\theta}$ the gradient descent solution $\hat{\theta} = P_\perp(\theta_0) + \Sigma^+ X^T Y$, and $\theta_0 \sim \mathcal{N}(0, \frac{1}{N} I)$. Then,

$$\begin{aligned}
 \text{Var}_{\theta_0}(h(x)) &= \mathbb{E}_{\theta_0}[(h(x) - \mathbb{E}_{\theta_0}[h(x)])^2] \\
 &= \mathbb{E}_{\theta_0}[x^T (P_\perp(\theta_0) - \mathbb{E}_{\theta_0}[P_\perp(\theta_0)])^2] \\
 &= \text{Var}_{\theta_0}(x^T P_\perp(\theta_0)) \\
 &= \text{Var}_{\theta_0}(P_\perp(x)^T P_\perp(\theta_0)) \\
 &= \frac{1}{N} \|P_\perp(x)\|^2
 \end{aligned}$$

Since $\mathbb{E}_{\theta_0}(h(x)) = x^T \Sigma^+ X^T Y$, the calculation of $\text{Var}_\epsilon(\mathbb{E}_{\theta_0} h(x))$ is similar as in [D.1](#), where Σ^{-1} is replaced by Σ^+ . Thus,

$$\text{Var}_\epsilon(\mathbb{E}_{\theta_0} h(x)) = \sigma_\epsilon^2 \text{Tr}(xx^T \Sigma^+)$$

Taking the expected value over the empirical distribution, \hat{p} , of the sample, we find an explicit dependence on $r = \text{rank}(X)$, not N :

$$\begin{aligned}
 \mathbb{E}_{x \sim \hat{p}}[\text{Var}(h(x))] &= 0 + \mathbb{E}_{x \sim \hat{p}}[\sigma_\epsilon^2 \text{Tr}(xx^T \Sigma^+)] \\
 &= \sigma_\epsilon^2 \text{Tr}(\mathbb{E}_{x \sim \hat{p}}[xx^T] \Sigma^+) \\
 &= \sigma_\epsilon^2 \text{Tr}\left(\frac{1}{m} \Sigma \Sigma^+\right) \\
 &= \sigma_\epsilon^2 \frac{1}{m} \text{Tr}(I_r^+) \\
 &= \sigma_\epsilon^2 \frac{r}{m}
 \end{aligned}$$

where I_r^+ denotes the diagonal matrix with 1 for the first r diagonal elements and 0 for the remaining $N - r$ elements. □

D.3. Proof of Theorem 1

First we state some known concentration results ([Ledoux, 2001](#)) that we will use in the proof.

Lemma 1 (Levy). *Let $h : S_R^n \rightarrow \mathbb{R}$ be a function on the n -dimensional Euclidean sphere of radius R , with Lipschitz constant L ; and $\theta \in S_R^n$ chosen uniformly at random for the normalized measure. Then*

$$\mathbb{P}(|h(\theta) - \mathbb{E}[h]| > \epsilon) \leq 2 \exp\left(-C \frac{n\epsilon^2}{L^2 R^2}\right) \quad (11)$$

for some universal constant $C > 0$.

Uniform measures on high dimensional spheres approximate Gaussian distributions (Ledoux, 2001). Using this, Levy's lemma yields an analogous concentration inequality for functions of Gaussian variables:

Lemma 2 (Gaussian concentration). *Let $h : \mathbb{R}^n \rightarrow \mathbb{R}$ be a function on the Euclidean space \mathbb{R}^n , with Lipschitz constant L ; and $\theta \sim \mathcal{N}(0, \sigma \mathbb{I}_n)$ sampled from an isotropic n -dimensional Gaussian. Then:*

$$\mathbb{P}(|h(\theta) - \mathbb{E}[h]| > \epsilon) \leq 2 \exp\left(-C \frac{\epsilon^2}{L^2 \sigma^2}\right) \quad (12)$$

for some universal constant $C > 0$.

Note that in the Gaussian case, the bound is dimension free.

In turn, concentration inequalities give variance bounds for functions of random variables.

Corollary 1. *Let h be a function satisfying the conditions of Theorem 2, and $\text{Var}(h) = \mathbb{E}[(h - \mathbb{E}[h])^2]$. Then*

$$\text{Var}(h) \leq \frac{2L^2 \sigma^2}{C} \quad (13)$$

Proof. Let $g = h - \mathbb{E}[h]$. Then $\text{Var}(h) = \text{Var}(g)$ and

$$\text{Var}(g) = \mathbb{E}[|g|^2] = 2\mathbb{E} \int_0^{|g|} t dt = 2\mathbb{E} \int_0^\infty t \mathbb{1}_{|g|>t} dt \quad (14)$$

Now swapping expectation and integral (by Fubini theorem), and by using the identity $\mathbb{E} \mathbb{1}_{|g|>t} = \mathbb{P}(|g| > t)$, we obtain

$$\begin{aligned} \text{Var}(g) &= 2 \int_0^\infty t \mathbb{P}_R(|g| > t) dt \\ &\leq 2 \int_0^\infty 2t \exp\left(-C \frac{t^2}{L^2 \sigma^2}\right) dt \\ &= 2 \left[-\frac{L^2 \sigma^2}{C} \exp\left(-C \frac{t^2}{L^2 \sigma^2}\right) \right]_0^\infty = \frac{2L^2 \sigma^2}{C} \end{aligned}$$

□

We are now ready to prove Theorem 1. We first recall our assumptions:

Assumption 1. *The optimization of the loss function is invariant with respect to $\theta_{\mathcal{M}\perp}$.*

Assumption 2. *Along \mathcal{M} , optimization yields solutions independently of the initialization θ_0 .*

We add the following assumptions.

Assumption 3. *The prediction $h_\theta(x)$ is L -Lipschitz with respect to $\theta_{\mathcal{M}\perp}$.*

Assumption 4. *The network parameters are initialized as*

$$\theta_0 \sim \mathcal{N}(0, \frac{1}{N} \cdot I_{N \times N}). \quad (15)$$

We first prove that the Gaussian concentration theorem translates into concentration of predictions in the setting of Section 5.2.1.

Theorem 2 (Concentration of predictions). *Consider the setting of Section 5.2 and Assumptions 1 and 4. Let θ denote the parameters at the end of the learning process. Then, for a fixed data set, S we get concentration of the prediction, under initialization randomness,*

$$\mathbb{P}(|h_\theta(x) - \mathbb{E}[h_\theta(x)]| > \epsilon) \leq 2 \exp\left(-C \frac{N\epsilon^2}{L^2}\right) \quad (16)$$

for some universal constant $C > 0$.

Proof. In our setting, the parameters at the end of learning can be expressed as

$$\theta = \theta_M^* + \theta_{M^\perp} \quad (17)$$

where θ_M^* is independent of the initialization θ_0 . To simplify notation, we will assume that, at least locally around θ_M^* , M is spanned by the first $d(N)$ standard basis vectors, and M^\perp by the remaining $N - d(N)$. This will allow us, from now on, to use the same variable names for θ_M and θ_{M^\perp} to denote their lower-dimensional representations of dimension $d(N)$ and $N - d(N)$ respectively. More generally, we can assume that there is a mapping from θ_M and θ_{M^\perp} to those lower-dimensional representations.

From Assumptions 1 and 4 we get

$$\theta_{M^\perp} \sim \mathcal{N}\left(0, \frac{1}{N} I_{(N-d(N)) \times (N-d(N))}\right). \quad (18)$$

Let $g(\theta_{M^\perp}) \triangleq h_{\theta_M^* + \theta_{M^\perp}}(x)$. By Assumption 3, $g(\cdot)$ is L -Lipschitz. Then, by the Gaussian concentration theorem we get,

$$\mathbb{P}(|g(\theta_{M^\perp}) - \mathbb{E}[g(\theta_{M^\perp})]| > \epsilon) \leq 2 \exp\left(-C \frac{N\epsilon^2}{L^2}\right). \quad (19)$$

□

The result of Theorem 1 immediately follows from Theorem 2 and Corollary 1, with $\sigma^2 = 1/N$:

$$\text{Var}_{\theta_0}(h_\theta(x)) \leq C \frac{2L^2}{N} \quad (20)$$

Provided the Lipschitz constant L of the prediction grows more slowly than the square of dimension, $L = o(\sqrt{N})$, we conclude that the variance vanishes to zero as N grows.

D.4. Bound on classification error in terms of regression error

In this section we give a bound on classification risk $\mathcal{R}_{\text{classif}}$ in terms of the regression risk \mathcal{R}_{reg} .

Notation. Our classifier defines a map $h : \mathcal{X} \rightarrow \mathbb{R}^k$, which outputs probability vectors $h(x) \in \mathbb{R}^k$, with $\sum_{y=1}^k h(x)_y = 1$. The classification loss is defined by

$$\begin{aligned} L(h) &= \text{Prob}_{x,y}\{h(x)_y < \max_{y'} h(x)_{y'}\} \\ &= \mathbb{E}_{(x,y)} I(h(x)_y < \max_{y'} h(x)_{y'}) \end{aligned} \quad (21)$$

where $I(a) = 1$ if predicate a is true and 0 otherwise. Given trained predictors h_S indexed by training dataset S , the classification and regression risks are given by,

$$\mathcal{R}_{\text{classif}} = \mathbb{E}_S L(h_S), \quad \mathcal{R}_{\text{reg}} = \mathbb{E}_S \mathbb{E}_{(x,y)} \|h_S(x) - Y\|_2^2 \quad (22)$$

where Y denotes the one-hot vector representation of the class y .

Proposition 2. *The classification risk is bounded by four times the regression risk, $\mathcal{R}_{\text{classif}} \leq 4\mathcal{R}_{\text{reg}}$.*

Proof. First note that, if $h(x) \in \mathbb{R}^k$ is a probability vector, then

$$h(x)_y < \max_{y'} h(x)_{y'} \implies h(x)_y < \frac{1}{2}$$

By taking the expectation over x, y , we obtain the inequality $L(h) \leq \tilde{L}(h)$ where

$$\tilde{L}(h) = \text{Prob}_{x,y}\{h(x)_y < \frac{1}{2}\} \quad (23)$$

We then have,

$$\begin{aligned} \mathcal{R}_{\text{classif}} &:= \mathbb{E}_S L(h_S) \leq \mathbb{E}_S \tilde{L}(h_S) \\ &= \text{Prob}_{S; x,y}\{h_S(x)_y < \frac{1}{2}\} \\ &= \text{Prob}_{S; x,y}\{|h_S(x)_y - Y_y| > \frac{1}{2}\} \\ &\leq \text{Prob}_{S; x,y}\{\|h_S(x) - Y\|_2 > \frac{1}{2}\} \\ &= \text{Prob}_{S; x,y}\{\|h_S(x) - Y\|_2^2 > \frac{1}{4}\} \leq 4\mathcal{R}_{\text{reg}} \end{aligned}$$

where the last inequality follows from Markov's inequality. □

E. Common intuitions from impactful works

“Neural Networks and the Bias/Variance Dilemma” from (Geman et al., 1992): “How big a network should we employ? A small network, with say one hidden unit, is likely to be biased, since the repertoire of available functions spanned by $f(x; w)$ over allowable weights will in this case be quite limited. If the true regression is poorly approximated within this class, there will necessarily be a substantial bias. On the other hand, if we overparameterize, via a large number of hidden units and associated weights, then the bias will be reduced (indeed, with enough weights and hidden units, the network will interpolate the data), but there is then the danger of a significant variance contribution to the mean-squared error. (This may actually be mitigated by incomplete convergence of the minimization algorithm, as we shall see in Section 3.5.5.)”

“An Overview of Statistical Learning Theory” from (Vapnik, 1999): “To avoid over fitting (to get a small confidence interval) one has to construct networks with small VC-dimension.”

“Stability and Generalization” from Bousquet & Elisseeff (2002): “It has long been known that when trying to estimate an unknown function from data, one needs to find a tradeoff between bias and variance. Indeed, on one hand, it is natural to use the largest model in order to be able to approximate any function, while on the other hand, if the model is too large, then the estimation of the best function in the model will be harder given a restricted amount of data.” Footnote: “We deliberately do not provide a precise definition of bias and variance and resort to common intuition about these notions.”

Pattern Recognition and Machine Learning from Bishop (2006): “Our goal is to minimize the expected loss, which we have decomposed into the sum of a (squared) bias, a variance, and a constant noise term. As we shall see, there is a trade-off between bias and variance, with very flexible models having low bias and high variance, and relatively rigid models having high bias and low variance.”

“Understanding the Bias-Variance Tradeoff” from Fortmann-Roe (2012): “At its root, dealing with bias and variance is really about dealing with over- and under-fitting. Bias is reduced and variance is increased in relation to model complexity. As more and more parameters are added to a model, the complexity of the model rises and variance becomes our primary concern while bias steadily falls. For example, as more polynomial terms are added to a linear regression, the greater the resulting model’s complexity will be.”

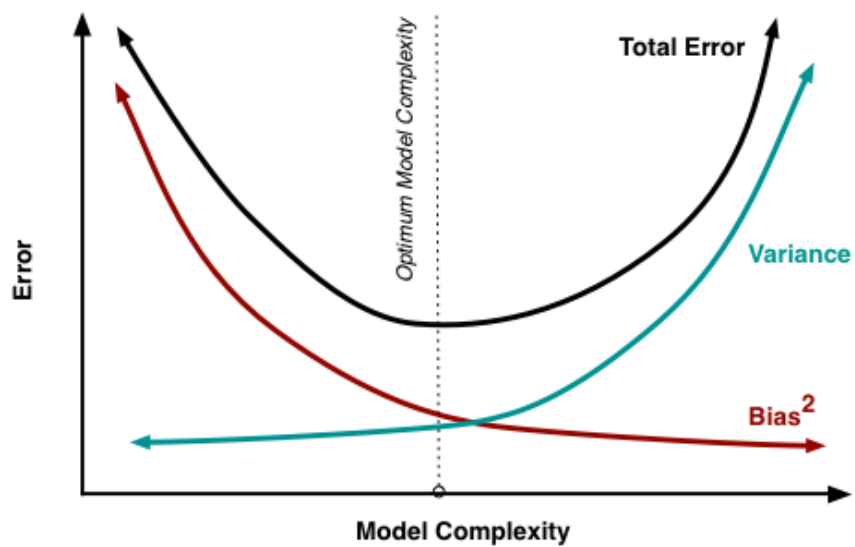


Figure 21: Illustration of common intuition for bias-variance tradeoff (Fortmann-Roe, 2012)